JACS
JOURNAL OF THE AMERICAN CHEMICAL SOCIETY
Communication
pubs.acs.org/JACS

Structural Transitions in Nanoparticle Assemblies Governed by Competing Nanoscale Forces

Rachelle M. Choueiri,[†] Anna Klinkova,[†] Héloïse Thérien-Aubin,[‡] Michael Rubinstein,*[,§] and Eugenia Kumacheva*[,†,‡,∥]

[†]Department of Chemistry, University of Toronto, 80 Saint George Street, Toronto, Ontario M5S 3H6, Canada

[‡]Department of Chemical Engineering and Applied Chemistry, University of Toronto, 200 College Street, Toronto, Ontario M5S 3E5, Canada

[§]Department of Chemistry, University of North Carolina, Chapel Hill, North Carolina 27599-3290, United States

[∥]The Institute of Biomaterials and Biomedical Engineering, University of Toronto, 4 Taddle Creek Road, Toronto, Ontario M5S 3G9, Canada

Supporting Information

ABSTRACT: Assembly of nanoscale materials from nanoparticle (NP) building blocks relies on our understanding of multiple nanoscale forces acting between NPs. These forces may compete with each other and yield distinct stimuli-responsive self-assembled nanostructures. Here, we report structural transitions between linear chains and globular assemblies of charged, polymer-stabilized gold NPs, which are governed by the competition of repulsive electrostatic forces and attractive poor solvency/hydrophobic forces. We propose a simple quantitative model and show that these transitions can be controlled by the quality of solvent, addition of a salt, and variation of the molecular weight of the polymer ligands.

Ensembles of inorganic nanoparticles (NPs) show collective electronic, optical and magnetic characteristics that originate from the coupling of size- and shape-dependent properties of individual NPs.[1,2] A cost-efficient approach to the fabrication of nanoscale materials utilizes the self-assembly of NP building blocks and yields a broad range of nanostructures—from small clusters to large three-dimensional (3D) lattices.[3,4] Control over the size and shape of these assemblies relies on our understanding of the nanoscale forces acting between NPs.[5] Examples of such forces include dipole−dipole interactions,[6] electrostatic forces,[7] hydrogen bonding,[8] hydrophobic,[9] coordination[10] and biospecific forces.[11] Attractive and repulsive interactions between NPs may change in magnitude and compete, depending on environmental factors.

Generation of different types of nanostructures from the same type of NPs offers a route to the fabrication of stimuli-responsive nanomaterials. Typically, this strategy relies on regio-specific attachment of distinct ligands to NP surface. For example, gold and semiconductor nanorods capped with different molecules along their long side and at the tips behave as amphiphilic molecules and organize in a variety of structures, when the quality of the solvent is selectively reduced for a particular ligand type.[4,12] Site-specific attachment of distinct ligands to the NP surface is achieved due to their preferential binding to a particular crystalline facet,[13] which may be challenging for small, close-to-spherical NPs and/or the use of macromolecular ligands. A more beneficial approach to distinct self-assembled nanostructures would rely on stimulus-dependent competition of nanoscale forces.

Here we report this approach by controlling structural transitions between two distinct types of nanostructures: linear and 3D assemblies of charged, polymer-stabilized gold NPs. The transitions were governed by the competition of attractive hydrophobic/poor solvency forces and repulsive electrostatic forces, and were achieved by varying the composition and ionic strength of the solvent or the molecular weight of the polymer ligands.

Small, spherical 23 nm-diameter gold NPs stabilized with cetyltrimethylammonium bromide were subjected to ligand exchange with thiol-terminated polystyrene (PS) molecules, as described elsewhere.[14] The number average molecular weights of the PS ligands used in the present work were 5×10^3, 1.2×10^4, 2×10^4, 3×10^4 and 5×10^4 g/mol (later in the text referred to as PS-5K, PS-12K, PS-20K, PS-30K and PS-50K, respectively). Following ligand exchange, the NPs were redispersed in *N*,*N*-dimethylformamide (DMF). A solution of NPs in DMF was colloidally stable for at least, 5 months.

The self-assembly of the NPs was induced by adding various amounts of water to the solution of NPs in DMF, thereby reducing the quality of solvent for the PS ligands.[15] To screen unfavorable interactions between the solvent and the PS molecules, the NPs associated in various types of structures. We observed three types of species formed in the colloidal solution when the content of water, C_w, in the DMF/water mixture and the molecular weight, M_n, of the PS ligands were changed, namely, individual NPs, spherical 3D NP clusters (globules), and linear NP chains with occasional branches (Figure 1). For a particular range of C_W and M_n, coexistence of chains and globules of NPs was observed. The self-assembly of the NPs was "mapped" by a phase-like diagram in the M_n-C_w parameter space. The diagram in Figure 2 shows the transitions between individual NPs (I), globules (G) and NP chains (C), as well as a narrow G + C range. No self-assembly occurred for the NPs

Received: May 1, 2013
Published: June 27, 2013

dx.doi.org/10.1021/ja404341r | J. Am. Chem. Soc. 2013, 135, 10262−10265

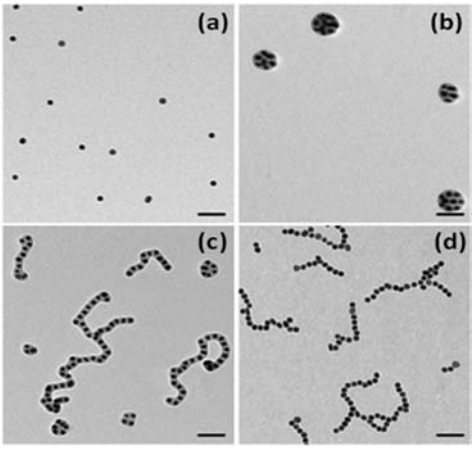

Figure 1. Transmission electron microscopy (TEM) images of the representative NP species after adding of water to the colloidal NP solution in DMF. (a) Individual NPs stabilized with PS-5K at C_w = 5 vol. %. (b) Globules of NPs stabilized with PS-50K at C_w = 5 vol.%. (c) Mixture of chains and globules of NPs stabilized with PS-50K at C_w = 10 vol.%. (d) Chains of NPs stabilized with PS-5K at C_W = 15 vol.%. The scale bars are 100 nm. The self-assembly time t_{SA} is 1 h.

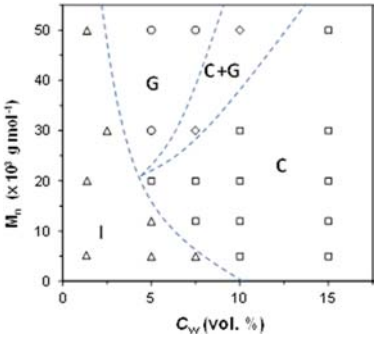

Figure 2. Phase-like diagram of the self-assembled structures of gold NPs, plotted in the M_n−C_w space. t_{SA}= 1 h. A transition from self-assembled structures (globules or chains) to individual NPs was achieved with either sonication for 15 min or heating of the system at 40 °C for 4 h (see Supporting Information). The diagram was constructed by analyzing TEM images.

stabilized with low-molecular weight PS and/or in the low C_w range. The ability of NPs to form globules vs. chains was determined by the interplay of M_n and C_w. At high M_n (≥30000) and low C_w the formation of globules was favored, whereas for higher content of water (dependent on M_n), NP chains were the dominant species. The transition G → C was not sharp and occurred via a regime, in which both of the species were present.

We carried out a detailed study of the NP chains and globules. The globular assemblies were similar to 3D clusters that were formed in tetrahydrofuran by PS-stabilized gold NPs.[16] Similar to this earlier report, in our work, NP globules assembly in solution could be monitored by dynamic light scattering and could be quenched by encapsulating the globules with a polystyrene-*block*-poly(acrylic acid) copolymer. The hydrodynamic diameter of the globules measured after self-assembly time, t_{SA}, of 1 h in the DMF/water mixture was 102.5 ± 1.5 nm, in comparison with 32.8 ± 3.4 nm, measured for individual NPs in DMF solution (Figure 3a).

With increasing concentration of water in the DMF/water mixture, the diameter of the globules (determined by analyzing

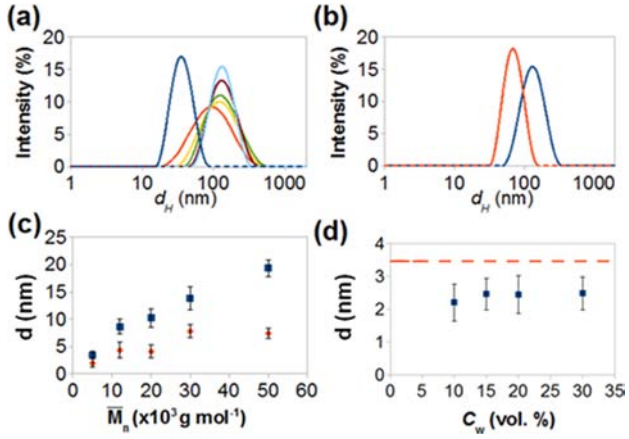

Figure 3. (a) Variation in the hydrodynamic diameter of the globules formed by NPs capped with PS-50K at C_w =7.5 vol. %, measured at t_{SA} of 0, 20, 30, 40, 50, and 60 min, shown with blue, red, yellow, green, violet, and light blue curves, respectively. (b) Hydrodynamic diameters of globules obtained from NPs stabilized with PS-50K at C_w = 5 vol. % (red curve) and at C_w = 7.5 vol.% (blue curve). (c) Variation in interparticle distance in the chains at C_w = 15 vol. % (red diamonds) and in the close-packed arrays of NPs dried on the TEM grid at C_w = 0 (blue squares), plotted as a function of M_n of PS ligands. (d) Variation in interparticle spacing plotted vs. C_w in the DMF/water mixture for the chains formed by NPs stabilized with PS-5K. The dashed red line shows the corresponding interparticle distance in close-packed arrays dried on the TEM grid at C_w = 0.

TEM images) increased from ∼72 nm (C_w = 5 vol. %) to ∼84 nm (C_w = 7.5 vol. %). The corresponding change in the hydrodynamic radius of the globules (determined in dynamic light scattering experiments) is shown in Figure 3b.

Chains of NPs grew in a marked similarity to step-growth polymerization, with the average number of NPs in the chains increasing linearly with time, similar to our earlier work on the self-assembly of gold nanorods.[17,18] The average distance, d, between the NPs in the chains increased with the molecular weight of PS ligands (Figure 3c), consistent with a larger polymer volume localized in the gap between the NPs. The same trend was observed for the dense NP arrays obtained by drying their solution in DMF on the TEM grid. For such arrays, the interparticle distance was consistently larger than that in the chains (Figure 3c), due to the more extended vitrified conformation of PS ligands in a good solvent. For 10 ≤ C_w ≤ 30 vol. %, interparticle distance did not significantly change (Figure 3d), in agreement with our earlier work.[14]

The structural transitions shown in Figure 2 were reversible. For example, for NPs stabilized with PS-50k, the C → I and G → I transformations occurred when the concentration of water in the system was reduced to ∼2 vol. %. Importantly, the C→ I transition occurred via the globular state, as shown in the phase diagram in Figure 2.

The structural transitions between NP chains and globules were rationalized as follows. The resultant structure of NP assemblies was determined by the minimization of the total energy of the system, ΔE_t, governed by the contributions of attraction forces (favoring a compact globular structure) and repulsion forces (favoring the formation of chains) as

$$\Delta E_t = \Delta E_{el} + \Delta E_h \quad (1)$$

In eq 1, ΔE_{el} is the change in energy of repulsive electrostatic interactions and ΔE_h is the change in energy representing a

dx.doi.org/10.1021/ja404341r | J. Am. Chem. Soc. 2013, 135, 10262−10265

combined effect of hydrophobic/poor solvency attraction forces (later in the text referred to as "hydrophobic forces"). We ignored attractive short-range van der Waals interactions, since over the entire range of interparticle separations hydrophobic forces dominated. A weak contribution of van der Waals forces was also supported by the absence of association of PS-stabilized NPs at low content of water in the DMF/water mixture.

Figure 4a and b illustrates the configurations formed by three adjacent NPs in the chains and globules, respectively. The type of structure was determined by the angle θ between the lines connecting the center of the second NP with the centers of adjacent 1st and 3rd NPs. The value of θ changed from 60° (the globular shape) to 180° (the chain shape).

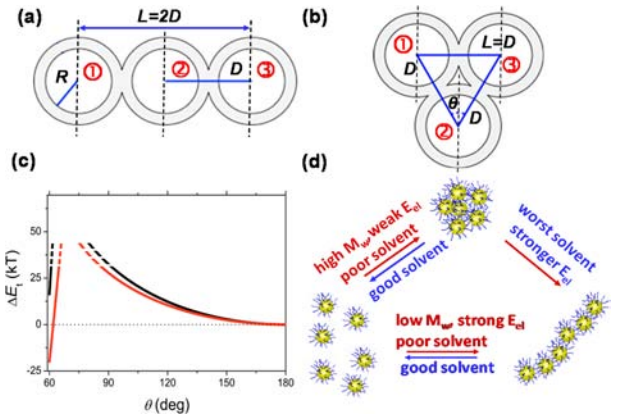

Figure 4. (a,b) Schematics of three neighboring NPs in the chain (a) and in the globule (b). The inner and outer circles illustrate the metal Au cores and the PS shells, respectively. For notations see Supporting Information. (c) Change in the total energy of the system with angle θ between the lines connecting the center of the second NP with the centers of the 1-st and 3-d NPs (shown in b). Red and black lines correspond to the DMF/water mixtures with C_w of 5 and 15 vol.%, respectively. The energy barrier between the globular and chain configurations is to be determined. (d) Schematic of the structural transitions in NP ensembles.

The change in energy of attraction upon NP association was calculated as

$$\Delta E_h = \Delta E_{st} = \gamma \times \Delta A \quad (2)$$

where ΔE_{st} is the reduction in the surface energy when two NPs form contact, γ is the interfacial tension between the collapsed PS ligands and the DMF/water mixture, and ΔA is the change in area of this interface when two NPs associate.

The change in electrostatic energy for two associating NPs in the absence of added salt was calculated using the approximation developed for charged spherical NPs functionalized with polymer brushes[19] as a logarithmic function of the surface-to-surface interparticle distance as

$$\Delta E_{el} = \frac{\pi^2}{2}\frac{kT}{l_B}R\ln\left(\frac{2D-2R}{L-2R}\right) \quad (3)$$

where R is the radius of the gold core of the NP; D is the center-to-center distance between the two neighboring PS-coated NPs; L is the center-to-center distance between the 1st and the 3rd PS-coated NPs (equal to 2D and D for θ of 180 and 60°, respectively), as shown in Figure 4a,b; k is the Boltzmann constant and T is the absolute temperature. In eq 3, l_B is the Bjerrum length ($=e^2/\varepsilon kT$), the distance at which the total interaction potential of counterions is equal to the thermal energy kT, where e is the elemental charge and ε is the dielectric constant of the solvent. The NP configuration at θ = 180° was chosen as a reference. Thus eq 3 shows a logarithmic dependence of the electrostatic energy as a function of the surface-to-surface separation between NPs with respect to the 180° configuration, with separation between surfaces 2D-2R.

We evaluated the variation in ΔE_t for the assembly of NPs stabilized with PS-50K in two solvent DMW/water mixtures at C_w of 5 and 15 vol.%, in which the NPs assembled into the globules and the chains, respectively. For calculations, we used R = 11.5 nm, and ε of 40 and 49[20] (corresponding to l_B of 1.14 and 1.4 nm, respectively), and γ of 1.4×10^{-3} J/m^2 to 1.9×10^{-3} J/m^2 for C_w of 5 and 15 vol.%, respectively. The derivation of eq 3 and details of the calculations are given in Supporting Information.

Figure 4c shows the variation in ΔE_t for two solvent compositions. For C_w = 5 vol.%, the NP configuration with a minimum in ΔE_t at θ = 60° was favored (corresponding to NP globules), due to the stronger contribution of the surface energy. For C_w = 15 vol.%, the deeper minimum in ΔE_t was achieved at θ = 180° (corresponding to NP chains), due to the larger contribution of electrostatic repulsion. Both predictions were in agreement with experimental results. We note that individually, both types of nanostructures have been reported for gold NPs, although in different systems. Chains were observed for charged gold NPs stabilized with low-molecular-weight ligands,[21,22] while the "non-directional" attraction between PS- or DNA-capped gold NPs led to the formation of 3D lattices.[3]

The schematic in Figure 4d summarizes the structural transitions in assemblies of gold NPs. Poor solvency conditions in conjunction with strong electrostatic repulsion yielded NP chains. Poor solvency conditions and weak electrostatic forces yielded globules. Improvement in the quality of solvent and reduction in E_{el} led to the C → G transition. When the quality of solvent was not sufficiently reduced, the NPs existed as individual species. Reduction in the quality of solvent did not lead to G → I transitions, because of the kinetic trapping of globular structures (see Figure S6b, Supporting Information).

We note that in the self-assembly experiments, the addition of water to the NP solution in DMF increased (although at a different rate) both E_h and E_{el}, due to the reduction in solvent quality for the PS ligands and the increase in solvent polarity, respectively. To validate the argument about competing E_h and E_{el}, we conducted NP self-assembly in the DMF/water mixture in the presence of NaCl. The addition of NaCl to the DMF/water mixture reduced the quality of solvent for the PS ligands[23] and suppressed the electric double layer interactions of the NPs,[24] thus favoring "non-directional" hydrophobic forces and the formation of globules. This trend is shown in Table 1: with increasing content of NaCl in the DMF/water mixture, C → G transitions took place, with an intermediate regime, in which both species were present.

The competition between the hydrophobic and electrostatic forces was further demonstrated by adding tetrahydrofuran (THF) to the NP solution in the DMF/water mixture at THF/DMF volume ratios of $0.1 \le \phi_{THF/DMF} \le 1$. Since the Flory–Huggins interaction parameters for PS-DMF and PS-THF solutions are 0.46 and 0.4, respectively,[21,25,26] in the presence of THF, the quality of the solvent for the PS ligands was improved. Thus, the hydrophobic interactions between the PS-

dx.doi.org/10.1021/ja404341r | J. Am. Chem. Soc. 2013, 135, 10262–10265

Table 1. Effect of the Addition of NaCl and THF on NP Assembly[a]

	C_{NaCl} (mM)			$\varphi_{THF/DMF}$		
	10	50	300	0.1	0.5	1
Structure	C	C+G	G	C+G	G	G

[a]NaCl and THF were added to the DMF/water solution of NPs stabilized with PS-50K at C_W = 15 vol. %.

coated NPs in the DMF/THF/water solution were weaker than in the DMF/water mixture. On the other hand, the addition of THF reduced the polarity of the mixed solvent (the dielectric constant of THF is 7.5[27]), thereby suppressing electrostatic interactions between the NPs. With increasing ratio $\phi_{THF/DMF}$ in the solution, the structure of NP assemblies changed from globules + chains ($\phi_{THF/DMF}$ = 0.1, ε = 42) to globules ($\phi_{THF/DMF}$ = 1, ε = 31) (Table 1).

To conclude, we have demonstrated reversible structural transitions in assemblies of polymer-coated gold NPs. We show that by tuning the delicate balance between the hydrophobic and electrostatic forces, assembly of NPs in two distinct configurations—3D globules or linear chains—can be achieved. A particular nanostructure can be realized in several ways: by tuning solvent polarity, by adding a salt, and by varying the molecular weight of the polymer ligands. Since the formation of chain or globular assemblies was governed by the interaction of ligands, rather than affected by the nature of the gold core, we hypothesize that the reported behavior is general and similar transitions can be expected for other types of charged NPs coated with polymer ligands.

■ ASSOCIATED CONTENT

Supporting Information

Synthesis of gold NPs, description of self-assembly experiments, tests of the reversibility of the structural transitions, the description of interfacial tension measurements and calculations of the change of total energy of the system. This material is available free of charge via the Internet at http://pubs.acs.org.

■ AUTHOR INFORMATION

Corresponding Author

ekumache@chem.utoronto.ca; mr@unc.edu

Notes

The authors declare no competing financial interest.

■ ACKNOWLEDGMENTS

E.K., R.C., A.K., and H.T.-A. thank NSERC Canada (Strategic Network Grant and Discovery grant) for financial support of this work. M.R. acknowledges support from the National Science Foundation under grants CHE-0911588, DMR-0907515, DMR-1121107, and DMR-1122483, the National Institutes of Health under 1-P5-HL107168, 1-P01-HL108808-01A1 and the Cystic Fibrosis Foundation. A.K. acknowledges Ontario Trillium Scholarship. R.C. thanks I. Gourevich for help with TEM imaging.

■ REFERENCES

(1) (a) Nie, Z.; Petukhova, A.; Kumacheva, E. *Nat. Nanotech.* **2010**, *5*, 15−25. (b) Wang, L.; Xu, L.; Kuang, H.; Xu, C.; Kotov, N. A. *Acc. Chem. Res.* **2012**, *45*, 1916−1926. (c) Romo-Herrera, J. M.; Alvarez-Puebla, R. A.; Liz-Marzán, L. M. *Nanoscale* **2011**, *4*, 1304−1315.

(2) (a) Gao, Y.; Tang, Z. *Small* **2011**, *7*, 2133−2146. (b) Carbone, C.; et al. *Adv. Funct. Mater.* **2011**, *21*, 1212−1228. (c) Xu, L.; Kuang, H.; Xu, C.; Ma, W.; Wang, L.; Kotov, N. A. *J. Am. Chem. Soc.* **2012**, *134*, 1699−1709.

(3) (a) Nykypanchuk, D.; Maye, M. M.; Van Der Lelie, D.; Gang, O. *Nature* **2008**, *451*, 549−552. (b) Park, S. Y.; Lytton-Jean, A. K. R.; Lee, B.; Weigand, S.; Schatz, G. C.; Mirkin, C. A. *Nature* **2008**, *451*, 553−556.

(4) (a) Petukhova, A.; Greener, J.; Liu, K.; Nykypanchuk, D.; Nicolaÿ, R.; Matyjaszewski, K.; Kumacheva, E. *Small* **2012**, *8*, 731−737. (b) Zhao, N.; Liu, K.; Greener, J.; Nie, Z.; Kumacheva, E. *Nano Lett.* **2009**, *8*, 3077−3081. (c) Zhao, N.; Vickery, J.; Guerin, G.; Park, J. I.; Winnik, M. A.; Kumacheva, E. *Angew. Chem., Int. Ed.* **2011**, *50*, 4606−4610. (d) Fava, D.; Nie, Z.; Winnik, M. A.; Kumacheva, E. *Adv. Mater.* **2008**, *20*, 4318−4322.

(5) Min, Y.; Akbulut, M.; Kristiansen, K.; Golan, Y.; Israelachvili, J. *Nat. Mater.* **2008**, *7*, 527−538.

(6) Thomas, J. R. *J. Appl. Phys.* **1966**, *37*, 2914−2915.

(7) Kalsin, A. M.; Fialkowski, M.; Paszewski, M.; Smoukov, S. K.; Bishop, K. J. M.; Grzybowski, B. A. *Science* **2006**, *312*, 420−424.

(8) Mayer, C. R.; Neveu, S.; Secheresse, F.; Cabuil, V. *J. Colloid Interface Sci.* **2004**, *273*, 350−355.

(9) Rasch, M. R.; Rossinyol, E.; Hueso, J. L.; Goodfellow, B. W.; Arbiol, J.; Korgel, B. A. *Nano Lett.* **2010**, *10*, 3733−3739.

(10) Si, S.; Raula, M.; Paira, T. K.; Mandal, T. K. *ChemPhysChem.* **2008**, *9*, 1578−1584.

(11) Caswell, K. K.; Wilson, J. N.; Bunz, U. H. F.; Murphy, C. J. *J. Am. Chem. Soc.* **2003**, *125*, 13914−13915.

(12) Figuerola, A.; et al. *Adv. Mater.* **2009**, *21*, 550−554.

(13) Murphy, C. J.; Sau, T. K.; Gole, A. M.; Orendorff, C. J.; Gao, J.; Gou, L.; Hunyadi, S. E.; Li, T. *J. Phys. Chem. B.* **2005**, *109*, 13857−13870.

(14) Nie, Z. H.; Fava, D.; Kumacheva, E.; Zou, S.; Walker, G. C.; Rubinstein, M. *Nat. Mater.* **2007**, *6*, 609−614.

(15) Brandrup, J.; Immergut, E. H.; Grulke, E. A. *Polymer Handbook*, 4th ed.; Wiley and sons: New York, 1999.

(16) Sánchez-Iglesias, A.; et al. *ACS Nano* **2012**, *6*, 11059−11065.

(17) Liu, K.; Nie, Z.; Zhao, N.; Li, W.; Rubinstein, M.; Kumacheva, E. *Science* **2010**, *329*, 197−200.

(18) Lee, A.; Andrade, G. F. S.; Ahmed, A.; Souza, M. L.; Coombs, N.; Tumarkin, E.; Liu, K.; Gordon, R.; Brolo, A. G.; Kumacheva, E. *J. Am. Chem. Soc.* **2011**, *133*, 7563−7570.

(19) Zhulina, E. B.; Boulakh, A. B.; Borisov, O. V. *Z. Phys. Chem.* **2012**, *226*, 625−643.

(20) Kumbharkhane, A. C.; Puranik, S. M.; Mehrotra, S. C. J. *Solution Chem.* **1993**, *22*, 219−229.

(21) Zhang, H.; Wang, D. *Angew. Chem., Int. Ed.* **2008**, *47*, 3984−3987.

(22) Yang, M.; Chen, G.; Zhao, Y.; Silber, G.; Wang, Y.; Xing, S.; Han, Y.; Chen, H. *Phys. Chem. Chem. Phys.* **2010**, *12*, 11850−11860.

(23) Liu, K.; Resetco, C.; Kumacheva, E. *Nanoscale* **2012**, *4*, 6574−6580.

(24) Israelachvili, J. N. *Intermolecular and Surface Forces*; Acad. Press: San Diego, CA, 2011.

(25) Wolf, B. A.; Willms, M. M. *Makromol. Chem.* **1978**, *179*, 2265−2277.

(26) Schulz, G. V.; Baumann, H. *Makromol. Chem.* **1968**, *114*, 122−138.

(27) Franks, F., Ed. *Water, A Comprehensive Treatise*; Plenum Press: New York, 1973; Vol. 2, Ch. 7.